Exp Brain Res (1990) 79:271–282

Experimental Brain Research

Functional organization of the cortical 17/18 border region in the cat

Y.-c. Diao [1], W.-g. Jia [2]*, N.V. Swindale [2]*, and M.S. Cynader [2]*

[1] Institute of Biophysics, Academia Sinica, Beijing 100080, China
[2] Department of Psychology, Dalhousie University, Halifax B3H 4J1, Canada

Summary. The representation of the visual field in the 17/18 border region of the cat's visual cortex, and the layout of orientation and ocular dominance columns, were studied by making many closely spaced electrode penetrations into the superficial layers of the flattened dorsal region of the marginal gyrus and recording response properties at each location. The 17/18 border region was defined by measuring the change in the horizontal component of receptive field position within the gyrus: as the position of the recording electrode moved from medial to lateral, the receptive fields moved towards the vertical midline, indicating that the electrode was in area 17; as penetrations were made in increasingly lateral positions, the trend reversed, and receptive field positions moved away from the midline, indicating that the electrode was in area 18. The receptive fields of cells close to the border straddled, or lay within 2°–3° on either side of the vertical midline. In addition, patches of cortex were sometimes encountered in which cells had receptive field centers located up to 7° in the ipsilateral visual field. Experiments in which maps were made in the left and right hemispheres of a single animal showed that these patches had a complementary distribution in the two hemispheres. Cells within the patches behaved as though driven by Y-cell inputs: they usually had large receptive fields and responded to rapidly-moving stimuli. They were broadly tuned for orientation and strongly dominated by the contralateral eye. Fourier spectral analysis of orientation selectivity maps showed that iso-orientation bands had an average spacing of 1.14 ± 0.1 mm and tended to be elongated in a direction orthogonal to the 17/18 border. Individual bands crossed the border without obvious interruption, although singularities (points of discontinuity in the layout of orientations) were more frequently observed in the border region than in adjacent areas. Two dominant periodicities could be measured in the maps of ocular dominance, one at around 0.8 ± 0.2 mm and a second at 2.0 ± 0.3 mm. No constant direction of elongation was noted. These are close to the periods present within areas 17 and 18 respectively.

Key words: Visual cortex – 17/18 border – Retinotopic map – Orientation map – Ocular dominance map – Cat

Introduction

The organisation of the border region between areas 17 and 18 of the cat is of interest for a number of reasons. First, the border includes the central visual field representation (Hubel and Wiesel 1962, 1965, 1967; Whitteridge 1973; Tusa et al. 1978, 1979) from which the animal obtains detailed information about its visual environment. Second, in addition to other afferent and efferent connections, this region receives and sends out heavy callosal projections (Garey et al. 1968; Zeki 1970; Berlucchi 1972; Innocenti 1980; Segraves and Rosenquist 1982), and hence must be involved in interhemispheric exchanges of visual information. Third, the question of how transitions occur between maps of functional properties in adjacent cortical areas is of interest. The 17/18 border of the cat, unlike many other cortical borders which are embedded in the depths of sulci, is largely found on the surface-flattened dorsal part of the visual cortex and is therefore easily approached.

* Present address: Department of Ophthalmology, University of British Columbia, 2550 Willow Street, Vancouver, British Columbia V5Z 3N9, Canada

Offprint requests to: Y.-c. Diao, Beijing (address see above)

Data relevant to these questions can be obtained from studies of area 17 and area 18 (for example, Garey et al. 1968; Hubel and Wiesel 1962, 1965; Tretter et al. 1975; Albus 1975a, b; Hubel et al. 1978; Humphrey and Norton 1980; Humphrey et al. 1985; Horton and Hubel 1981; Singer 1981; Berman et al. 1982; Albus and Sieber 1984; Cynader et al. 1987; Löwel et al. 1987; Löwel and Singer 1987) and from studies on the function of the corpus callosum (for example, Hubel and Wiesel 1967; Shatz 1977; Innocenti 1980; Blakemore et al. 1983; Payne et al. 1984; Cynader et al. 1986; Gardner and Cynader 1987). Few experiments however have been specially designed to investigate the functional organization of this region. In a series of experiments, in which data were collected from oblique penetrations passing successively through V1 (area 17) and V2 (area 18), Orban et al. (1980) and Orban (1984) found an order shift at the 17/18 transition zone in response strength, velocity characteristics and direction selectivity, and suggested that these changes might be used for tracing the 17/18 border between successively recorded cells. However, precise determination of the border is not easy due to the gradual nature of change of these parameters.

Other investigators have used anatomical methods to study and compare organisation in areas 17 and 18. Using a flat-mount technique combined with 2-deoxyglucose autoradiography or with transneuronal autoradiography, Löwel et al. (1987) and Löwel and Singer (1987) studied, respectively, the global morphological features of orientation columns and ocular dominance columns in the two areas, and found that orientation bands and the elongated ocular dominance patches tended to run normal to the 17/18 border. These results were consistent with earlier anatomical studies (Albus and Sieber 1984; Singer 1981; Shatz et al. 1977) and suggestions based on oblique and long distance recordings and 2-DG studies of the striate cortex of the tree shrew (Humphrey and Norton 1980; Humphrey et al. 1985).

In this study we investigated the layout of orientation preference and ocular dominance in relation to the 17/18 border region of the cat, as defined by the position of the reversal or reflection of the retinotopic map that occurs about the visual midline. Our methods were similar to those used by Cynader et al. (1987) and consisted of making physiological recordings of orientation preference, ocular dominance, receptive field position and receptive field size from each of a large number of closely spaced penetrations in the superficial layers of the cortex on either side of the (presumed) border region. The resulting data were then subjected to various sorts of analysis, including calculation of Fourier power spectra of ocular dominance and orientation values, and completion (i.e. interpolation) of the different maps using appropriate kinds of local averaging (Cynader et al. 1987; Swindale et al. 1987).

Methods

Fourteen normal adult cats weighing 2.5–3 kg were used in the study; 12 of these animals yielded a total of 14 maps which were used for data analysis. Preparation and recording procedures were similar to those used by Cynader et al. (1987). Before anesthetizing the animal, a dose of dexagen (0.3 mg dexamethasone, s.c.) was injected to prevent brain edema. The animal was then anesthetized with i.v. injection of sodium pentobarbital, as required. Atropine sulphate was given (i.v.) to decrease salivation. After tracheal cannulation, the animal was placed in a stereotaxic device which allowed unobstructed vision. During recording, light anesthesia was maintained by artificially ventilating the animal with a mixture of N_2O and O_2 (70:30). A muscle relaxant, gallamine triethiodide (10 mg/kg/h), and dextrose in Ringer (10 cc/h) as well as supplementary sodium pentobarbital (1 mg/kg/h) were continuously administered through a venous cannula. The long-lasting local anesthetic, marcaine, was applied to wound and pressure points. End-tidal pCO_2 was monitored and maintained at a level of 3.5–4% by adjusting the rate or volume (or both) of the respirator. Body temperature was kept at 38° C using a feedback-controlled heating pad. EKG and EEG were monitored. The eyes were treated with atropine to dilate the pupils, and phenylephrine eye-drops to retract the nictitating membranes. Contact lenses with a 4 mm artificial pupil were chosen by retinoscopy to focus the eyes on a tangent screen 145 cm distant in front of the animal.

An opening of the skull, about 7 × 12 mm in size, was made at the stereotaxic coordinates P0–P12, and L0–L7. Of the thus exposed rectangle of brain surface the 17/18 border roughly constituted the diagonal. In some cases, a larger opening (11 × 12 mm) was made to expose the 17/18 border regions of both hemispheres, which enabled us to record successively from both sides of the brain. After durotomy, a photomicrograph of the brain surface and a scale bar was taken with instant slide film, and the detailed blood vessel pattern was used as a guide for marking recording sites during the experiment, and later for calculating the coordinates of the penetrations. This made it possible to reduce coordinate reading errors caused by distortion of the cortex during the experiment (Cynader et al. 1987). A Davies chamber was mounted on the skull with dental acrylic cement and screws, and then filled with a transparent, viscous mineral oil. This substantially reduced pulsation of the brain caused by artificial ventilation and heartbeats, and allowed the electrode to be moved and to be seen through the transparent oil and the plexiglas roof of the chamber.

Platinum-iridium microelectrodes coated with glass were used for recording (Wolbarsht et al. 1960). The exposed tip length of the electrode was about 20–50 μm, tip diameter, 1–2 μm, and shaft diameter at a distance of 500 μm from the tip, 10 μm. The impedance of the electrodes ranged from 0.3 to 0.7 MΩ. With these electrodes single or multi-unit activity could easily be recorded yet no damage to the brain tissue was detected in histological sections when recording depth was limited to the superficial 700 μm of the cortex (Cynader et al. 1987).

To ensure accuracy in determining the position of the receptive fields relative to the area centralis we adopted three tactics: a) we usually plotted the response field (as defined by Barlow et al. 1967) and used the centre of the response field as the measure of receptive field position; b) we monitored residual movements of each eye by frequently re-plotting both the position of the area centralis and an easily recognisable retinal landmark, usually an intersection of two blood vessels more than 10° away from the area centralis. Subsequent measurements of receptive field position were then corrected for movements of the eyes. c) Since cyclotorsional eye movements that can occur under paralysis may result in differences between the mean separation of paired receptive fields and the horizontal separation of the areae centrales (Blakemore et al. 1983), we calculated and compared these two separations. The results showed that the angular difference of the two separations was minor, ranging from 0.5° to 1°.

Multi- and sometimes single unit responses were recorded at cortical depths between 400–700 μm, corresponding to layers II and III. Since the penetrations were always normal to the brain surface and the cortex has a columnar organization (Hubel and Wiesel 1962, 1974), the recorded units in any one penetration usually had similar response properties, including position in the visual field, orientation selectivity, and ocularity (Cynader et al. 1987). For a single map, usually about 150 penetrations with an average spacing of about 300 μm were made. For each penetration location, the coordinates of the recording sites on the brain surface, the location and size of the receptive field in each eye, optimal orientation and range of orientation selectivity, ocular dominance group (according to Hubel and Wiesel's (1962) scaling scheme), direction preference and optimal velocity of moving stimuli were determined and stored in a computer data file. Analysis of the stored data was carried out on an IBM-XT computer, using a series of specially designed MAP programs (Swindale et al. 1987). These analyses included: a) calculation of the iso-azimuth and iso-elevation contours within the retinotopic map by means of local averaging of receptive field position; b) calculation of a fine-grain orientation map from the initial coarse one; c) a similar calculation of a fine grain ocular dominance map and d) Fourier power spectrum analysis of the orientation and ocular dominance maps to detect regularity and periodicity of these two parameters.

Power spectrum values were calculated after carrying out a 2-dimensional fast Fourier transform of data values stored in a 64×64 array (Brigham 1974). Ocular dominance values were scaled (by subtraction of their mean value) so that their average value was zero before carrying out the transformation. This removes the d.c. (or zero) frequency component from the data, which would otherwise be large. Orientation values were represented as complex numbers with unitary modulus, doubling the orientation angle before resolving into real and imaginary components (Swindale et al. 1987).

Results

Penetrations were made in rows, starting either from the medial edge of the marginal gyrus and moving successively more lateral or, alternatively, were started on the lateral side and placed successively more medial. This was meant to ensure that each line of penetrations crossed the 17/18 border. Most of the recorded cells had complex receptive fields, with characteristics typical of those described by Hubel and Wiesel (1962, 1965). The majority were binocularly driven, and had ON-OFF responses to properly oriented stimuli. When the electrode was moved from medial to lateral across the cortex, many characteristics of the recorded cells changed. The most obvious difference, apart from the position of the receptive field, was an increase in receptive field size, and an increase in the optimal velocity for a moving stimulus. This is in accordance with the functional differences between areas 17 and 18 that have been described by other investigators (Hubel and Wiesel 1965; Tretter et al. 1975; Orban et al. 1980; Orban 1984).

The retinotopic map

All penetrations were carried out within an area in which cells had their receptive fields located no more than 10° of horizontal visual angle from the zero vertical meridian. The vertical extent of receptive field positions ranged from 1°–2° above the horizontal meridian to about 20° below. In this region the following general retinotopic rules were obeyed: the upper part of the visual field was represented by the caudal portion of the cortex, and the lower part of the visual field represented by the rostral portion of the cortex. As the electrode was moved from medial to lateral, starting from area 17, the average position of the receptive fields shifted from temporal to nasal in the visual field until a location at which the sequence of shifts reversed, and field location became progressively more temporal, indicating that the recording electrode was currently in area 18 (Tusa et al. 1978, 1979). It was generally necessary for the electrode to move more than a millimetre in distance across the cortex before such shifts became clearly apparent owing to the local scatter in receptive field positions (Hubel and Wiesel 1974).

The scatter of the receptive field positions, together with possible errors in plotting the receptive fields, made it difficult to determine the positions of iso-azimuth and iso-elevation contours within the cortical map. This problem was addressed with the assistance of a computer program which performed an interpolation operation based on local averaging of receptive field positions. Data values were first scaled and then entered into a two-dimensional array, with a resolution of typically 8 to 16 array points per cortical millimeter. For each point in the array the average of all receptive field positions lying within a circle of radius 0.45 mm was calculated. This was done for all positions for which four or more data points (i.e. penetrations) lay within the search radius. A second local

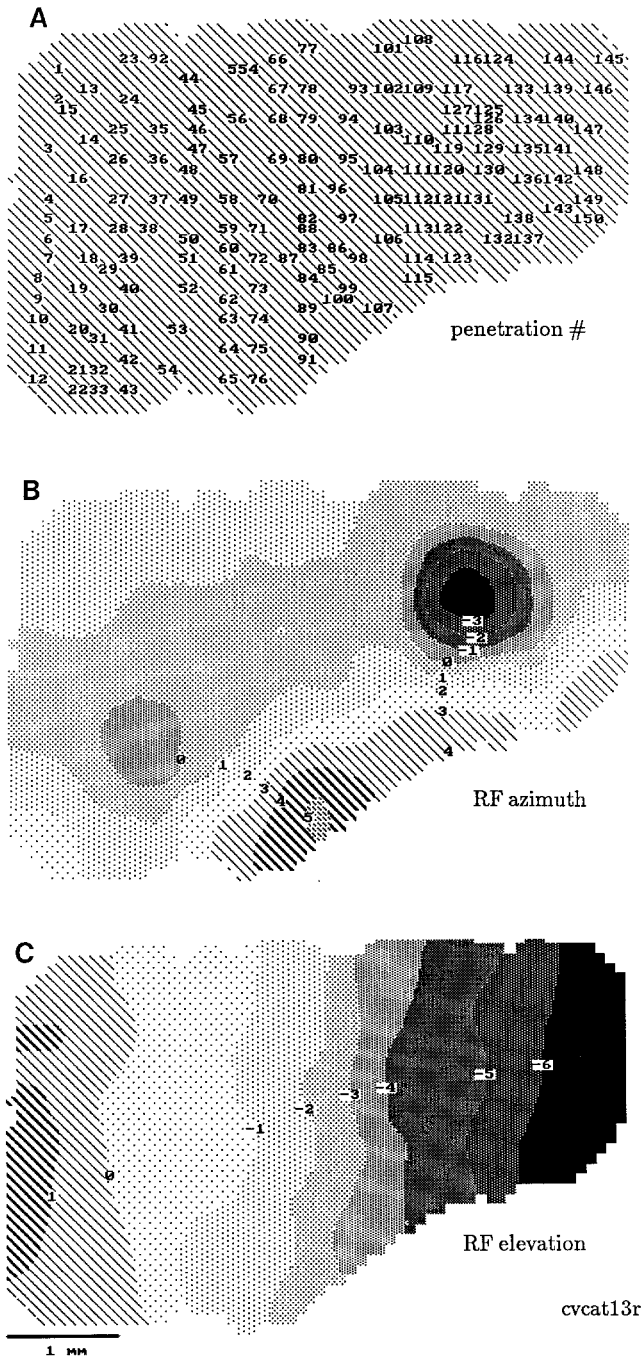

Fig. 1 A–C. Computer-generated retinotopic map of the 17/18 border region in the right hemisphere of cat 13. **A** Surface view of the border region. Numerals indicate recording sites in order of penetration. **B** Retinotopic map of the same region as in **A**, with different grey levels used to show regions of constant receptive field (RF) azimuth. Boundaries between grey levels occur for every degree of visual angle. Zero represents the vertical meridian, and negative values represent the ipsi-hemifield. **C** Retinotopic map of the same region as in **A** showing regions of constant receptive field elevation. Zero represents the horizontal meridian, and negative values represent the lower visual field. In all three panels, the anterior portion of the brain is to the right, and medial is toward the top. Scale bar in this and all subsequent figures = 1 mm

smoothing procedure (in which each point in the array was set equal to half its own value plus half the average value of its four nearest neighbors) was then repeated from 3–5 times to further remove variability from the interpolated retinotopic map. The resulting interpolated maps possessed relatively smooth iso-elevation and iso-azimuthal contours, and maintained reasonable fidelity to the measured data values.

Figure 1 illustrates the results of these procedures: panel A shows the array of penetrations in the right hemisphere in a typical map. Numerals indicate the order of penetrations. Panel B shows the calculated iso-azimuth contours from the same map, using different gray scales to represent intervals of 1° of azimuthal angle. For the purposes of subsequent analysis we defined the 17/18 border region as the area representing the ipsilateral visual field and the part of the contralateral visual field between 1° and the vertical meridian. As can be

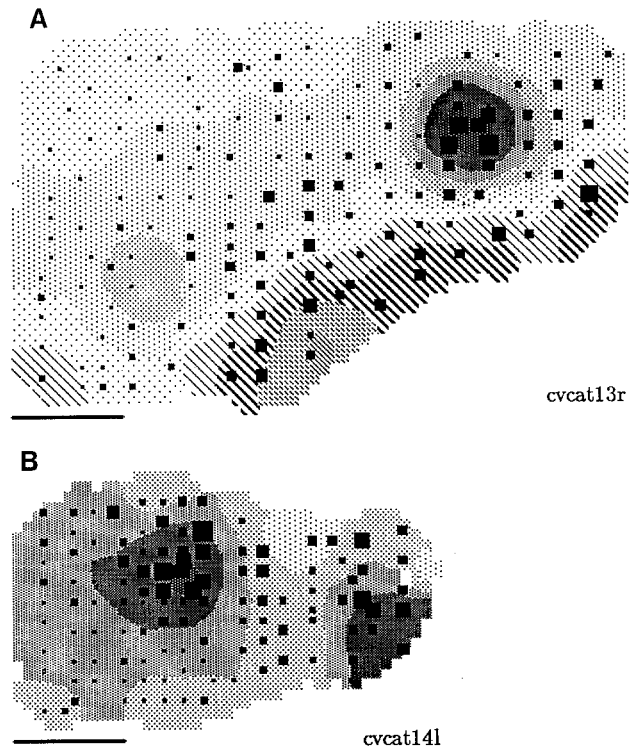

Fig. 2 A, B. Maps from two different animals (**A** and **B**) of the receptive field sizes in the 17/18 border region were superimposed on the azimuthal retinotopic maps to show regional differences of the receptive field size. Size of each filled square is proportional to the size of the receptive field measured as the diagonal length. Shading convention for representing receptive field azimuth is the same as in Fig. 1 B. Receptive fields vary in size from 1° (smallest squares) to 8° (largest squares). Scale bar = 1 mm; anterior is to the right, and medial is towards the top in both figures

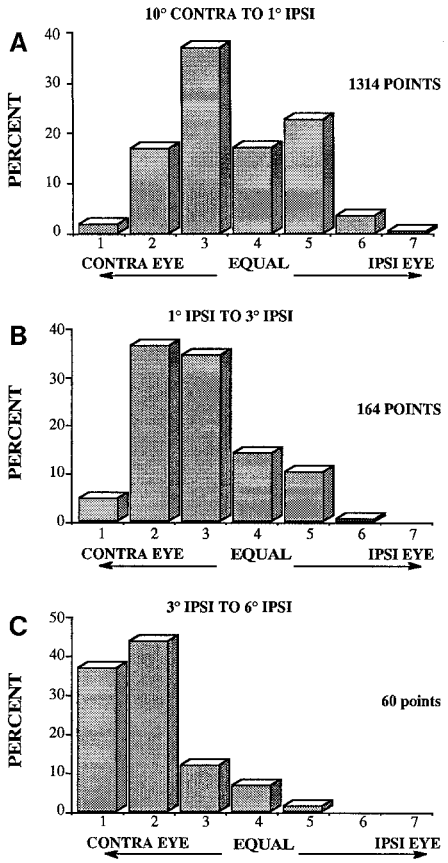

Fig. 3A–C. Comparisons of ocular dominance in areas representing different azimuthal angle sectors of the visual field according to Hubel and Wiesel's scheme for scaling. Data are taken from a total of 14 maps made in 12 animals

seen from Fig. 1 B, this is a strip 1–2 mm wide running from antero-medial to postero-lateral across the cortex. Panel C in Fig. 1 shows the calculated iso-elevation contours in the same map, also with an interval of 1° between regions with different shading. Comparing these two maps, one can see that equivalent visual angles in the central visual field are represented over a larger cortical area than those of the paracentral field. Thus, magnification changes with retinal eccentricity. In addition, magnification in elevation is generally larger than that in azimuth, as has been described for area 18 (Tusa et al. 1979; Cynader et al. 1987). However the magnification anisotropy is reduced over the area centralis representation. In the area representing about 1° of visual angle around the centre of the area centralis, no anisotropy is apparent.

A striking and consistent finding is that there are patches in the 17/18 border region in which recorded units have their receptive field centers in the ipsilateral visual field. This is demonstrated in Fig. 1 B, which shows two shaded regions in which average receptive field position is in the ipsilateral hemifield. Cells in these ipsi-field patches usually had broad orientation tuning curves, to the extent that they often responded to orientations orthogonal to the preferred one. They responded vigorously to fast moving stimuli ($\leq 300°$/sec). Two other prominent features of these cells were that their receptive fields were larger, on average, than those from cells outside the patches (Fig. 2) and the cells were overwhelmingly dominated by the contralateral eye although in the majority, input from the ipsilateral eye could be detected (Fig. 3).

In a map of about 6 mm × 4 mm in size, one or two such ipsilateral field patches were typically encountered. The most ipsilateral receptive field centers we ever recorded were −7.2° from the vertical midline. Variation was noted in the linear size of the ipsi-field patches, which ranged from about one to several hundred μm if only the area representing the ipsilateral hemifield more than 1° from the vertical meridian was considered. Variation was noticed also in the cortical coordinates of the ipsi-

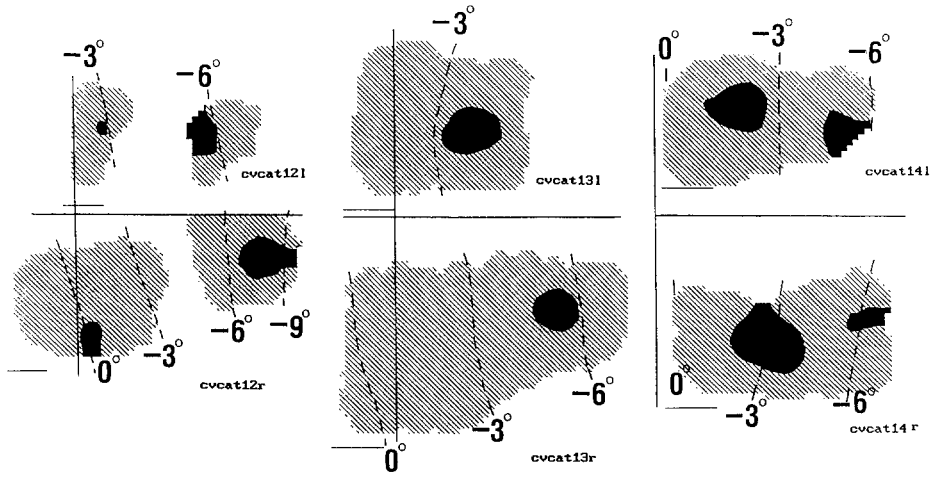

Fig. 4. Three examples of the distributions of ipsilateral visual field patches (shaded black) in pairs of maps made in the 17/18 border regions of the left and right hemispheres of the same animal. Dashed lines represent iso-azimuthal contours. The two sides of the brain are shown in register, as mapped, with 'O' indicating the intersection of the APO and MLO planes of the Horsley-Clark stereotaxic atlas. Note the complementary distribution of the patches in each hemisphere. Scale bars = 1 mm. Anterior is to the right in each case

lateral field zones, and in the location of the visual field represented. However, when we compared retinotopic maps obtained from corresponding areas in the two hemispheres of the same animal, we found that the ipsi-field patches were arranged complementarily in terms of visual field representation between the two sides of the brain. Figure 4 shows three examples of the arrangements of ipsi-field patches in the two opposite hemispheres and the part of visual field they represented.

The orientation selectivity map

At the border region almost all cells recorded at cortical depths of less than 700 μm (see Methods section) were orientation selective except for cells in the ipsi-field patches which, as noted above, often had poor orientation selectivity. As the electrode was moved from medial to lateral across the cortex, there was a gradual shift of preferred orientation. However, abrupt changes of preferred orientation were also frequently encountered.

To further study the map of preferred orientation the techniques developed by Swindale et al. (1987) were used. These allowed us to reconstruct a fine-grain map of orientation from the initial (relatively) coarse one obtained during the experiment. Briefly, the methodology involved representing orientation as a vector value before carrying out a Fourier based filtering operation (equivalent to interpolation) in which components of frequency in the orientation map higher than the sampling limit (imposed by the spacing of penetrations) were removed. This procedure has been shown to estimate the values of preferred orientation, for all points in the map, to within about 30° of the value that would have been measured had a penetration been made at that position (Swindale et al. 1987). Figures 5 and 6 show examples of the orientation selectivity maps obtained by applying this procedure to our data.

The upper panel (A) of Fig. 5 shows the map of preferred orientation from one experiment. Each point represents one recording site and the orientation preference of the recorded unit is indicated by the orientation of the short bar. The lower panel (B) of Fig. 5 is the complete orientation selectivity map obtained by interpolation. Each of the six gray levels represents an orientation range of 30° centered respectively on 0° (horizontal), 30°, 60°, 90° (vertical), 120° and 150°, with the shading becoming progressively lighter for each of the 6 ranges. Panel C of Fig. 5 shows for comparison the two-dimensional Fourier power spectrum of the orientation map shown in Fig. 5A. The inter-

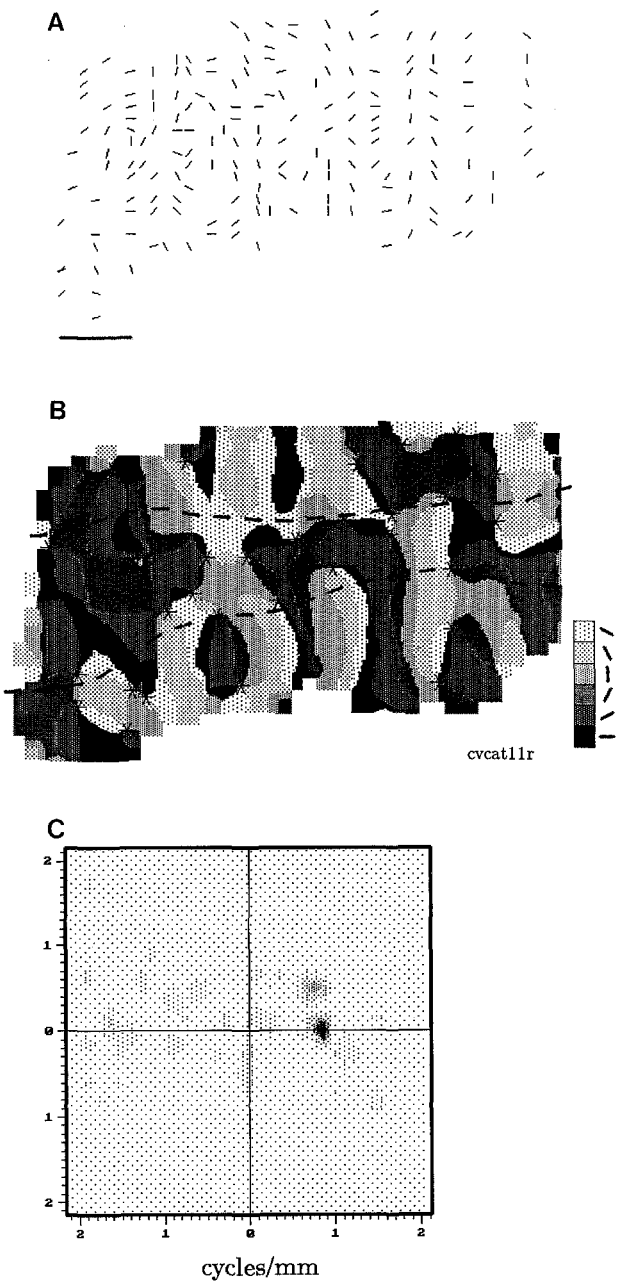

Fig. 5A–C. Computer-generated map of orientation preference in the right 17/18 border region of cat 11. **A** The raw orientation map. Each point represents one recording locus where the preferred orientation is indicated by a short bar. **B** The orientation map obtained after computer interpolation. The six gray levels represent, respectively, six different orientation ranges, each 30° wide. The darkest shading level represents horizontal orientation ±15°, and successively lighter shadings rotate in anticlockwise sequence from this. The border region, determined from the map of receptive field position, is demarcated by two dashed lines. Asterisks mark orientation singularities. Anterior is to the right and medial is toward the top. Scale bar = 1 mm. **C** The two-dimensional Fourier power spectrum obtained from the orientation map shown in A. There is a single energy peak located to the right of the origin at a frequency value of just under 1 cycle/mm. See text and legend to Fig. 8 for further explanation

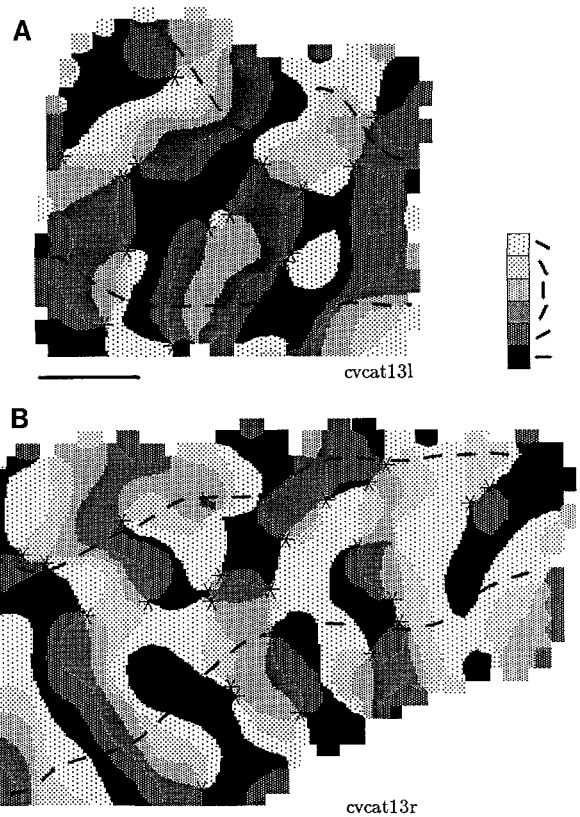

Fig. 6A, B. Orientation preference maps of the 17/18 border regions in the left and right hemispheres of cat 13. **A** Left hemisphere. **B** Right hemisphere. The dashed lines indicate the approximate location of the 17/18 border region as determined from the retinotopic map. Asterisks indicate orientation singularities. Anterior is to the right. Other conventions are the same as in Fig. 1 and 5. Note the complementary direction of elongation of the iso-orientation bands in the two hemispheres

pretation of this is described in more detail below, as well as in the legend to Fig. 8.

Figure 6 shows two more orientation maps. Panel A is a map from the right hemisphere, and panel B is from the corresponding area of the same animal's left hemisphere.

From Figs. 5 and 6 the following can be seen: the orientation selectivity map is composed of parallel bands that run from antero-lateral to postero-medial, and are thus approximately perpendicular to the 17/18 border strip (defined by the dashed lines) as predicted by morphological and other physiological methods (Albus 1979; Singer 1981; Albus and Sieber 1984; Cynader et al. 1987; Swindale et al. 1987; Löwel et al. 1987). Note that the directions of the bands in the two hemispheres are mirror symmetric. With movement across these bands the orientation shift may be in a clockwise or a counterclockwise direction. Although some bands are continuous, joining areas 17 and 18, most run only a short distance, meeting other bands at points referred to as singularities (Swindale et al. 1987). These points are marked with asterisks in the figures. Statistical calculations for 7 maps showed that the majority of a total of 115 singularities were in the border region, and that the density of singularities in this region ($2.972/mm^2$, $N=7$, SD ± 1.329) is significantly higher than that in the adjacent areas ($1.315/mm^2$, $N=7$, SD ± 0.733) with $P<0.01$.

The ocular dominance map

The map of ocular dominance in the 17/18 border region is different from that of orientation selectivity. When the electrode was moved from medial

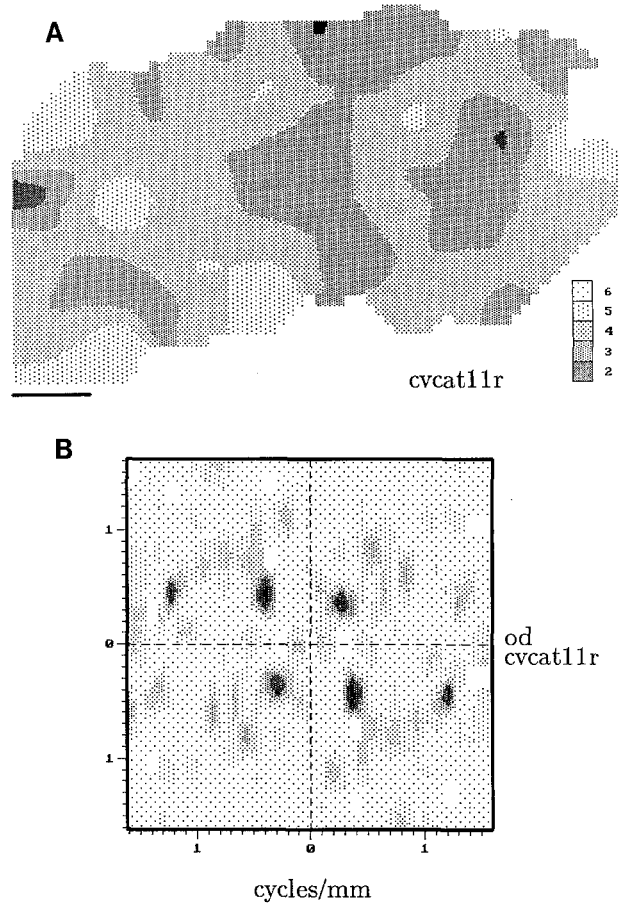

Fig. 7A, B. An interpolated ocular dominance map and its power spectrum. **A** Ocular dominance map in the right hemisphere of cat 11. Ocular dominance groups are indicated by different gray levels. Scale bar = 1 mm. **B** Two-dimensional Fourier power spectrum of the same ocular dominance map. Ordinates are in spatial frequency values (cycles per cortical millimeter); horizontal axis is frequency along the AP axis of the cortex; the vertical axis is frequency along the ML axis. Density of shading is proportional to the amount of energy present. (See text and legend to Fig. 8 for further explanation)

to lateral or in any other direction, the ocular preference changed gradually from one eye to the other and changed back again while the electrode was moved further. However more cells in the border region were dominated by the contralateral eye, and the period of the repetition of ocular dominance was not consistent. These features are reflected in the ocular dominance histograms of Fig. 3 and in the ocular dominance map produced by interpolation based on local averaging (similar to that used to calculate the retinotopic maps) as shown in panel A of Fig. 7. In Fig. 7A, each ocular dominance group is represented by a single grey level. It can be seen that the ocular dominance patches have irregular shapes and sizes. Some patches are elongated. The elongation may take any direction. Note that areas in which cells fell into group 3 constitute a large part of the whole map and join together to form a continuous one. Due to the nature of the interpolation operation, which removes variability, regions in which cells fell into groups 1, 6 and 7 are not represented since each of these regions makes up only a very small proportion of the map (see also Fig. 3).

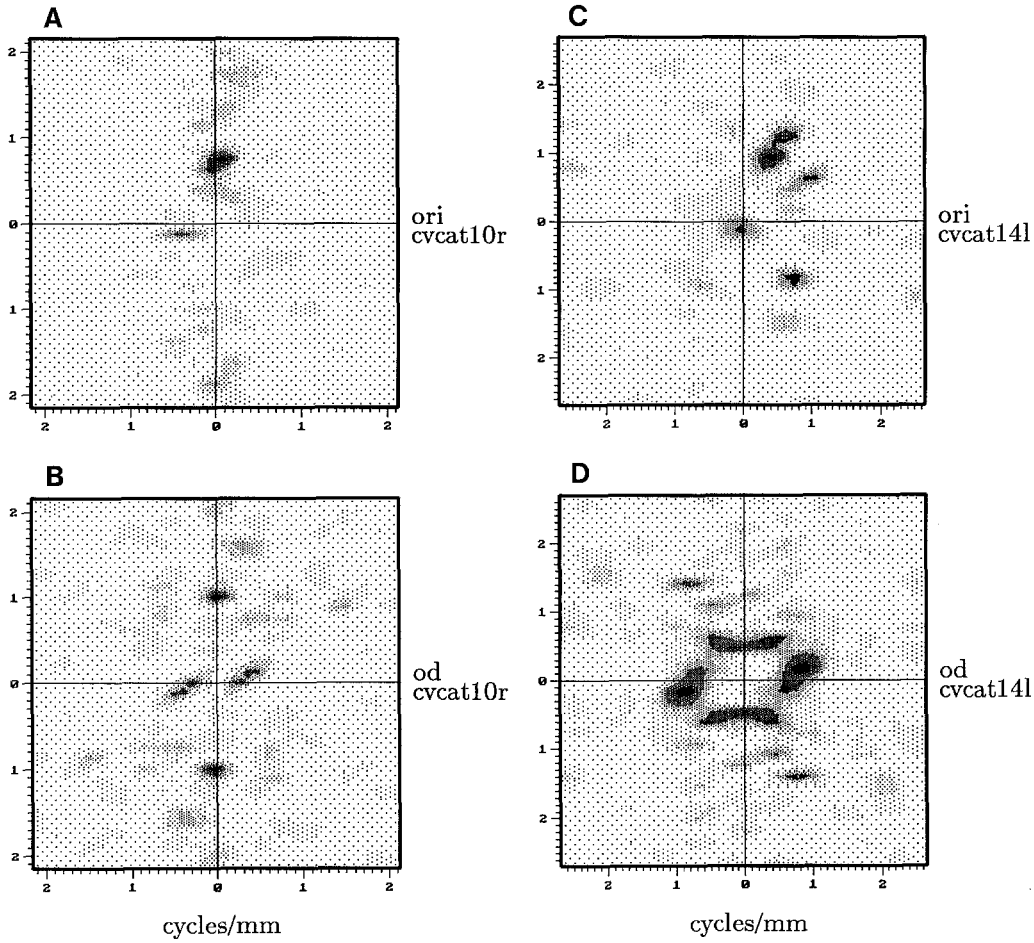

Fig. 8A–D. Fourier power spectra for orientation **A**, **C** and ocular dominance **B**, **D** in two representative animals. **A**, **B** Are from the same map, as are **C**, **D**. The X and Y axes represent spatial periodicity and are scaled in cycles per cortical millimeter. Shading level is proportional to the amount of energy present at a particular frequency. The *radial* distance of a peak from the origin indicates the presence of a dominant repeat period (i.e. spacing) of iso-orientation bands or ocular dominance patches. Thus the position of the peak in (**A**) indicates that the iso-orientation bands in this animal had a dominant periodicity of about 0.8 cycles/mm (or a wavelength of 1.25 mm). The direction of the peak relative to the origin – in this case nearly vertical – indicates that the iso-orientation bands run horizontally across the map (as represented on the page) which, in this figure, corresponds to the medio-lateral direction. Note that the ocular dominance spectra are symmetric (i.e. $E(x,y)=E(-x,-y)$ where E is energy and x and y are spatial periodicity coordinates). This is a mathematical consequence of the fact that ocular dominance is a scalar variable, unlike orientation which is a vector. Lack of symmetry in the orientation power spectrum indicates a tendency for the orientation map to be handed i.e. for orientation to change predominantly in a clockwise or anticlockwise direction for a given direction of movement (orthogonal to the direction of the bands) across the map. As far as we can tell, the degree of handedness varies randomly from one map to the next and does not depend on the side of the brain in which the map was made

Spectral analysis

To further assess the forms of organisation present in the maps of orientation and ocular dominance we carried out a two-dimensional Fourier spectral analysis of each property. Examples of this analysis, which was carried out in 14 different maps are shown in Figs. 5c, 7b and 8. The spectra typically contained one or more well defined energy peaks, at various distances from the origin. This *radial* distance is a measure of spatial frequency (scaled in cycles/mm in the figures). When these frequency values were measured for orientation they were found to be clustered around a single mean value of about 0.88 cycles/mm (Fig. 9). The values for ocular dominance however had a bimodal distribution, and were clustered around values of 0.5 and 1.4 cycles/mm (equivalent to wavelengths of 2.0 and 0.8 mm respectively; Fig. 9). This is not surprising, since ocular dominance is known to have different periodicities in areas 17 and 18 (Shatz et al. 1977; Swindale 1988). In a number of maps however, only one of these two frequency components was present, despite the fact that the maps straddled the border region. For each map therefore, it was possible to calculate an average orientation periodicity, and one or two values for ocular dominance periodicity. When these values were compared (Fig. 10) it was evident that in every case but one, ocular dominance periodicity was either higher or lower than the predominant orientation periodicity.

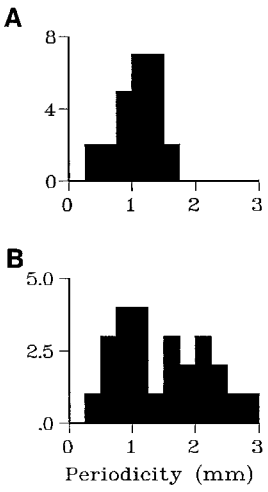

Fig. 9 A, B. Histograms of the periodicities of the peaks present in the orientation and ocular dominance power spectra from 14 maps obtained from 12 animals. Note that orientation periodicity (**A**) appears to be clustered around a single mean value, whereas ocular dominance periodicity (**B**) values have a bimodal distribution with peaks positioned either above or below that for orientation

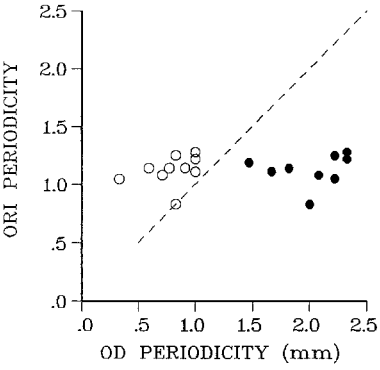

Fig. 10. For each map a single average orientation period was measured, together with either an upper or lower ocular dominance period (or both, if both were present). Each point in the graph shows the value for orientation graphed against the upper (*filled circles*) or lower (*open circles*) ocular dominance periodicity. Axes are scaled in wavelengths values (mm per cycle). The dashed line indicates equality between the two values. Note that the ocular dominance values lie on either side of the orientation period

The spectral analysis also yields information concerning the direction of elongation of ocular dominance patches or iso-orientation domains. When a single peak is present in the power spectrum (e.g. Fig. 5c) the direction of elongation is orthogonal to a line drawn between the peak and the origin. The position of the peak(s) in the orientation power spectra consistently indicated a tendency for iso-orientation bands to run approximately orthogonal to the 17/18 border as has been noted before. However, the spectra obtained from the ocular dominance maps were more complex, with different peaks subtending a variety of directions relative to the origin.

Discussion

Representation of the ipsilateral visual hemifield

Different experimental results have been reported concerning the representation of the ipsilateral visual field in areas 17 and 18 of the normal cat. Hubel and Wiesel (1962) and Tusa et al. (1978) noted about a 1.5° to 3° involvement of the ipsilateral hemifield when plotting the receptive fields of cells at the lateral boundary of area 17 in cats. However they attributed this ipsi-involvement to errors. Others, having adopted measures to reduce errors in plotting the receptive fields and in plotting the area centralis, reported an ipsi-hemifield involvement of no more than 1° or 2°. (Leicester 1968; Blakemore 1969; Orban et al. 1980; Berman et al. 1982) if only the receptive field centers were considered. On the other hand, Albus and Beck-

mann (1980) showed that there was about 5° of ipsilateral representation in area 18 when considering only the center of the receptive fields. Whitteridge and Clarke (1982) showed that on the 17/18 border there was a small region in which cells had their receptive fields centered up to 8°–12° in the ipsi-hemifield. Our results are in agreement with these earlier studies in showing that in the 17/18 border region most receptive fields are in the contralateral hemifield, straddle or lie in the ipsilateral hemifield near the vertical meridian. However, our finding of a patchy representation of receptive fields with centers as far as 7° in the ipsi-hemifield, and with a complementary distribution of patches in the two hemispheres, is new.

Three possible sources of error in studying the retinotopic map of the 17/18 border region should be considered first however. Firstly, the presence of residual eye movements in paralysed cats (Chow 1968; Bishop et al. 1971) could cause errors in receptive field localization. The magnitude of these movements in the present experiment was found to be 1° to 3°. We controlled for this by repeatedly plotting the area centralis and an easily identifiable intersection of two blood vessels and subsequently making necessary corrections of the position of plotted receptive field centers (Cynader et al. 1987). Secondly, because torsional eye movements may be induced by paralysis, the zero vertical meridian might not be truly vertical but tilted. To correct for this possible source of error we measured the mean separation of the two areae centrales and the mean separation of the two receptive fields for each binocular cell. Using the difference of these two separations, we were able to make further corrections (see Blakemore et al. 1983 for a fuller description), which usually amounted to no more than 1°. Thirdly, we could have erred in our estimate of the position of the area centralis. However we believe that our measurements of the location of area centralis, made with a reversible ophthalmoscope, are correct to within 1°–2°. We always took the geometric center of the retinal area devoid of blood vessels as the area centralis; this seemed in agreement with data deduced from the geometric relation between the area centralis and the optic disk (Bishop et al. 1962). In addition, it has been repeatedly reported that the ipsilateral representation of the visual field in area 17 of cat, in general, is about 1° to 2° when only the center of the receptive field is considered (Hubel and Wiesel 1967; Leicester 1968; Blakemore 1969; Tusa et al. 1978; Kato et al. 1978; Orban et al. 1980; Berman et al. 1982). These results have a firm anatomical base. Stone (1966) and Stone et al. (1978) have shown that the nasal and temporal portions of retina overlap along a vertical strip about 0.2 to 0.5 mm wide (equivalent to about 0.9° to 2.25° of visual angle). This is consistent with our results. When we moved the electrode mediolaterally across the 17/18 border, most of the reversals in the sequence of change in receptive field position occurred at places less than 1° from the vertical meridian. If the vertical meridian had been wrongly determined due to an incorrect estimation of the area centralis position, for example, if the vertical meridian had been drawn in the contralateral visual field, then most of the reversals would have occurred well before the receptive fields of recorded cells reached the vertical meridian, a situation which seems unlikely.

An ipsilateral field representation in the visual cortex has been found in the mouse (10°, Drager 1975), hamster (10°, Tiao and Blakemore 1976), and the sheep (10° to 15°, Clarke and Whitteridge 1976; Pettigrew et al. 1984). This ipsilateral representation may be functionally involved in binocular vision (Blakemore 1969; Whitteridge and Clarke 1982; Pettigrew et al. 1984). The ipsilateral field inputs have been suggested to arise via the corpus callosum (Blakemore 1969; Berlucchi 1972; Pettigrew et al. 1984), and also through the lateral geniculate nucleus (Whitteridge and Clarke 1982). By recording in both LGNds of the cat, Sanderson and Sherman (1971) have shown that in addition to a 3.5° overlap of receptive field centers in layer A and layer A1, which may derive from the central nasotemporal overlap of the retina (Stone 1966; Stone et al. 1978), another two overlaps exist in the C layers and in the medial interlaminar nucleus. These are mainly from the contralateral eye in which the centers of the receptive fields may extend up to 36° into the wrong hemifield. Recently, using intracellular HRP injection, Humphrey et al. (1985) were able to show that one LGN Y-cell axon had a receptive field in the ipsilateral hemifield. The fact that cells in the ipsi-field patches have large receptive fields, are dominated by the contralateral eye and respond to fast-moving stimuli, also suggests that the patches are largely driven by Y cell inputs.

It is difficult to think of a specific function for the ipsi-field patches. They seem to be rather widely spaced (2–4 mm) along the border, and represent no more than a few degrees of visual angle. However, if one considers the complementary arrangement of ipsi-field patches in the opposite hemispheres, the large receptive field of cells in the patches, and the existence of callosal connections between the two hemispheres it is possible that they could subserve a nearly complete and separate representation of the vertical midline.

The present study shows that in the 17/18 border region the overall periodicity of the iso-

orientation bands is similar to that within area 18. The average spacing of the orientation bands was found to be 1.14 ± 0.1 mm, only slightly less than the periodicity that was measured in area 18 using the same methodology (1.25 mm: Cynader et al. 1987; Swindale et al. 1987). Since measurements of orientation periodicity in area 17 seem to give slightly lower values (typically 1.0–1.1 mm) than in area 18 (Löwel et al. 1987; M. Cynader et al., unpublished), it is possible that orientation periodicity changes smoothly between the two areas. The same does not seem to be true for ocular dominance: studies of the layout of this property using trans-neuronal autoradiography show an approximately 2-fold difference in the periodicity of the bands in the two areas (Shatz et al. 1977; Anderson et al. 1988; Swindale 1988), and our spectral analysis data show that peaks at both the area 17 and 18 frequencies are present in the border region. Though interpretation of power spectral data is not straightforward, the presence of multiple energy peaks at a variety of orientations relative to the origin indicates that there may be complicated interactions at the border in terms of the distribution and shape or overall direction of elongation of the patches as the transition between frequencies is made.

In agreement with 2-deoxyglucose studies in the cat (Singer 1981; Löwel et al. 1987), physiological maps of area 18 (Cynader et al. 1987) in the cat, and studies using anatomical and physiological methods in the striate cortex of the tree shrew (Humphrey and Norton 1980; Humprey et al. 1985), the orientation bands run approximately normal to the 17/18 border. Although a few orientation bands run continuously across the border region, most bands run for only 1–2 mm. Statistical analysis shows that there are more singularities in the border region than in the adjacent area. It may not be a coincidence that in their 2-DG studies on the cat visual cortex, Löwel et al. (1987) found that the representation of the area centralis was always more lightly labeled, hence iso-orientation bands were less clear in this region than the rest of the cortex. This phenomenon may be accounted for if there are more singularities in this region, since they would tend to obscure the banded structure of the domains. Our findings are also supported by the observations of Albus (1979) who noted that iso-orientation domains revealed by 2-DG were less regular in form in regions of cortex near the vertical meridian representation. Albus (1975b) also noted the occurrence of discontinuous changes in orientation preference in tangential penetrations through the center of gaze representation in area 17, which is consistent with the present observations.

The orthogonal intersection of the orientation bands with the 17/18 border in the tree shrew has been used to suggest that the 17/18 border region is an organizing area during development (Humphrey et al. 1985). Our results support this hypothesis as well. The establishment of orientation selective bands may start at different points along the border in the same time window. Then the bands extend separately into area 17 and area 18. The role of the continuous bands which join areas 17 and 18 may be coordinative in the development of the orientation column system. However the opposite could be true as well: the bands might grow in towards the border with different periodicities, and then meet and join up as best as they can, resulting in a region with many singularities. However, there must be other reasons for the interruption of the bands since the singularities are not a unique characteristic of the border region.

Acknowledgements. Sohail Hasan took part in the initial stage of this study. This work was supported by NSERC and MRC of Canada, and in part by NSF of China.

References

Albus K (1975a) A quantitative study of the projection area of the central and paracentral visual field in area 17 of the cat. I. The precision of the topography. Exp Brain Res 24:159–179

Albus K (1975b) A quantitative study of the projection area of the central and paracentral visual field in area 17 of the cat. II. The spatial organization of the orientation domain. Exp Brain Res 24:181–202

Albus K, Beckmann R (1980) Second and third visual areas of the cat: interindividual variability in retinotopic arrangement and cortical location. J Physiol (Lond) 229:247–276

Albus K, Sieber B (1984) On the spatial arrangement of iso-orientation bands in the cat's visual cortical areas 17 and 18: a 14 C-deoxyglucose study. Exp Brain Res 56:384–388

Anderson PA, Olavarria J, Van Sluyters RC (1988) The overall pattern of ocular dominance bands in cat visual cortex. J Neurosci 8:2183–2200

Barlow HB, Blakemore C, Pettigrew JD (1967) The neural mechanism of binocular depth discrimination. J Physiol (Lond) 193:327–342

Berlucchi G (1972) Anatomical and physiological aspects of visual functions of corpus callosum. Brain Res 37:371–392

Berman N, Payne BR, Labar DR, Murphy EH (1982) Functional organization of neurons in cat striate cortex: variations in ocular dominance and receptive-field type with cortical laminae and location in the visual field. J Neurophysiol 48:1362–1377

Bishop PO, Kozak W, Vakkur GL (1962) Some quantitative aspects of the cat's eye: axes and planes of reference, visual field coordinates and optics. J Physiol 163:466–502

Bishop PO, Henry GH, Smith CJ (1971) Binocular interaction fields of single units in the cat striate cortex. J Physiol (Lond) 216:39–68

Blakemore C (1969) Binocular depth discrimination and the nasotemporal division. J Physiol (Lond) 205:471–497

Blakemore C, Diao Y-c, Pu M-l, Wang Y-k, Xiao Y-m (1983) Possible functions of the interhemispheric connections between visual areas in the cat. J Physiol 337:331–349

Brigham EO (1974) The fast Fourier transform. Prentice Hall, Englewood Cliffs, NJ
Chow KL (1968) Influence of residual eye movements in single unit studies of the visual system. Brain Res 8:385–388
Creutzfeldt OD, Innocenti GM, Brooks D (1974) Vertical organization in the visual cortex (area 17) of the cat. Exp Brain Res 21:315–336
Clarke PGH, Whitteridge D (1976) Cortical visual areas of the sheep. J Physiol (Lond) 256:497–508
Cynader M, Gardner J, Dobbins A, Lepore F, Guillemot JP (1986) Interhemispheric communication and binocular vision: functional and developmental aspects. In: Ptito M, Lepore F, Jasper HH (eds) Two hemispheres - one brain. Liss, New York
Cynader M, Swindale NV, Matsubara JA (1987) Functional topography in cat area 18. J Neurosci 7:1401–1413
Drager UC (1975) Receptive fields of single cells and topography in the mouse visual cortex. J Comp Neurol 160:269–190
Gardner JC, Cynader M (1987) Mechanisms for binocular depth sensitivity along the vertical meridian of the visual field. Brain Res 413:60–74
Garey LJ, Jones EG, Powell TPS (1968) Interrelationships of striate and extrastriate cortex with the primary relay sites of the visual pathway. J Neurol Neurosurg Psychiatr 31:135–157
Horton JC, Hubel DH (1981) Regular patchy distribution of cytochrome oxidase staining in primary visual cortex of macaque monkey. Nature 292:762–764
Hubel DH, Wiesel TN (1962) Receptive fields, binocular interaction and functional architecture in the cat's visual cortex. J Physiol (Lond) 160:106–154
Hubel DH, Wiesel TN (1965) Receptive fields and functional architecture in two nonstriate visual areas (18 and 19) of the cat. J Neurophysiol 28:229–289
Hubel DH, Wiesel TN (1967) Cortical and callosal connections concerned with the vertical meridian of the visual field in the cat. J Neurophysiol 30:1561–1573
Hubel DH, Wiesel TN (1974) Sequence regularity and geometry of orientation columns in the monkey striate cortex. J Comp Neurol 158:267–294
Hubel DH, Wiesel TN, Stryker MP (1978) Anatomical demonstration of orientation columns in macaque monkey. J Comp Neurol 177:361–379
Humphrey AL, Norton TT (1980) Topographic organization of the orientation column system in the striate cortex of the tree shrew (*Tupaia glis*). I. Microelectrode recording. J Comp Neurol 192:531–547
Humphrey AL, Sur M, Uhlrich DJ, Sherman SM (1985) Termination pattern of individual X- and Y-cell axons in the visual cortex of the cat: projections to area 18, to the 17/18 border region, and to both areas 17 and 18. J Comp Neurol 233:190–212
Innocenti GM (1980) The primary visual pathway through the corpus callosum: morphological and functional aspects in the cat. Arch Ital Biol 118:124–188
Kato H, Bishop PO, Orban GA (1978) Hypercomplex and simple/complex cell classifications in cat striate cortex. J Neurophysiol 41:1071–1095
Leicester J (1968) Projection of visual vertical meridian to cerebral cortex of the cat. J Neurophysiol 31:371–383
Löwel S, Singer W (1987) The pattern of ocular dominance columns in flat-mounts of the cat visual cortex. Exp Brain Res 68:661–666
Löwel S, Freeman B, Singer W (1987) Topographic organization of the orientation column system in large flat-mounts of the cat visual cortex: a 2-deoxyglucose study. J Comp Neurol 155:401–415
Orban GA (1984) Neuronal operations in the visual cortex. Studies of the brain function, Vol 11. Springer, Berlin Heidelberg New York Tokyo, pp 57–62
Orban GA, Kennedy H, Maes H (1980) Functional changes across the 17–18 border in the cat. Exp Brain Res 39:177–186
Payne BR, Pearson HE, Berman N (1984) Role of corpus callosum in functional organization of the cat striate cortex. J Neurophysiol 52:570–594
Pettigrew JD, Ramachandran VR, Bravo H (1984) Some neural connections subserving binocular vision in ungulates. Brain Behav Evol 24:65–93
Sanderson KJ, Sherman MS (1971) Nasotemporal overlap in visual field projected to lateral geniculate nucleus in the cat. J Neurophysiol 34:453–466
Segraves MA, Rosenquist AC (1982) The distribution of the cells of origin of callosal projections in cat visual cortex. J Neurosci 2:1079–1089
Shatz CJ (1977) Anatomy of interhemispheric connections in the visual system of Boston Siamese cats and ordinary cats. J Comp Neurol 173:497–518
Shatz CJ, Lindstrom S, Wiesel TN (1977) The distribution of afferents representing the right and left eyes in the cat's visual cortex. Brain Res 131:103–116
Singer W (1981) Topographic organization of orientation columns in the cat visual cortex: a deoxyglucose study. Exp Brain Res 44:431–436
Stone J (1966) The naso-temporal division of the cat's retina. J Comp Neurol 126:585–601
Stone J, Campson JE, Leicester J (1978) The naso-temporal division of retina in the Siamese cat. J Comp Neurol 180:783–798
Swindale NV (1988) Role of visual experience in promoting segregation of eye dominance patches in the visual cortex of the cat. J Comp Neurol 267:472–488
Swindale NV, Matsubara JA, Cynader MS (1987) Surface organization of orientation and direction selectivity in cat area 18. J Neurosci 7:1414–1427
Tiao Y-c, Blakemore C (1976) Functional organization in the visual cortex of the golden hamster. J Comp Neurol 168:459–482
Tretter F, Cynader M, Singer W (1975) Cat parastriate cortex: a primary or secondary visual area? J Neurophysiol 38:1099–1113
Tusa RJ, Palmer LA, Rosenquist AC (1978) The retinotopic organization of area 17 (striate cortex) in the cat. J Comp Neurol 177:213–236
Tusa RJ, Rosenquist AC, Palmer LA (1979) Retinotopic organization of areas 18 and 19 in the cat. J Comp Neurol 185:657–678
Whitteridge D (1973) Projection of optic pathways to the visual cortex. In: Jung R (ed) Handbook of sensory physiology, Vol VII/3. Central processing of visual information, Part B. Springer, Berlin Heidelberg New York, pp 247–268
Whitteridge D, Clarke PGH (1982) Ipsilateral visual field represented in the cat's visual cortex. Neuroscience 7:1855–1860
Wolbarsht MC, MacNicol EF, Wagner HG (1960) Glass insulated platinum microelectrode. Science 132:1309–1310
Zeki SM (1970) Interhemispheric connections of prestriate cortex in monkey. Brain Res 19:63–75

Received May 25, 1989 / Accepted August 21, 1989